Supplementary Information - Transition from viscoelastic to fracture-like peeling of pressure-sensitive adhesives

Marion Grzelka,[1, *] Stefan Kooij,[1] Sander
Woutersen,[2] Mokhtar Adda-Bedia,[3] and Daniel Bonn[1]

[1] *Van der Waals-Zeeman Institute, Institute of Physics,*
University of Amsterdam, 1098XH Amsterdam, The Netherlands

[2] *Van 't Hoff Institute for Molecular Science,*
University of Amsterdam, 1098XH Amsterdam, The Netherlands

[3] *Université de Lyon, Ecole Normale Supérieure de Lyon,*
Université Claude Bernard, CNRS,
Laboratoire de Physique, Lyon F-69342, France

* m.grzelka@uva.nl

I. YOUNG'S MODULUS OF THE BACKING OF THE TAPE

By peeling two layers of the adhesive over each other on an upside-down glass plate, we can track the peeling front but also the shape of the backing of the tape (Fig. S1 (a) and (b)). From the pictures, we extract the local angle α (Fig. S1(c)) as a function of the curvilinear abscissa s defined as:

$$ds\,\overrightarrow{t} = ds\cos(\alpha)\overrightarrow{e_x} + ds\sin(\alpha)\overrightarrow{e_y} \tag{1}$$
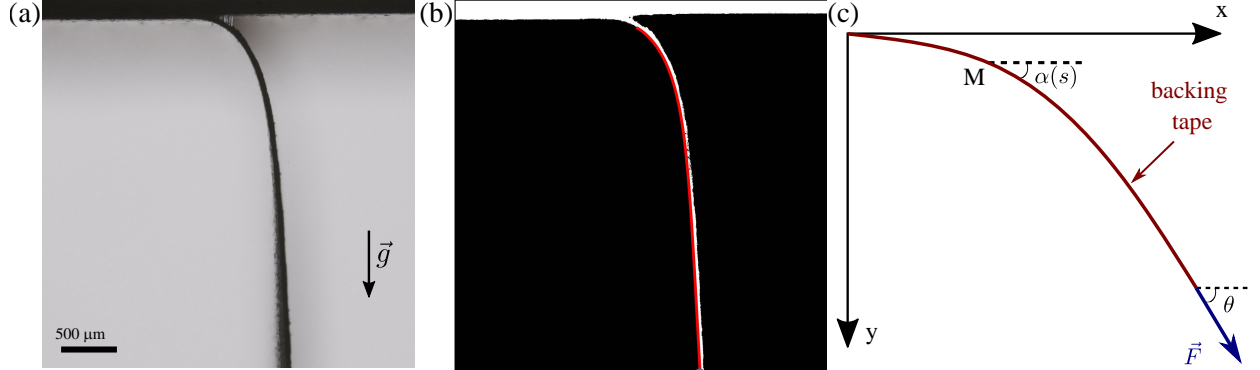

FIG. S1. Procedure to extract the backing profile of the tape. (a) Picture of the peeling of the Scotch tape (3M 810 Magic Scotch) at RH $= 12.5\%$ with a load $F = 803\,\mathrm{mN}$. (b) Binarization of the picture to extract the backing profile (red). (c) Illustration of the peeling. A load $\overrightarrow{F}$ is applied to the tape with a peeling angle θ. $\alpha(s)$ is the local angle in M.

Using simple elastica model for an inextensible beam [1], the local angle $\alpha(s)$ is:

$$\alpha(s) = \theta - 4\arctan\left(\tan\left(\frac{\theta}{4}\right)\exp\left(-\frac{s-s_0}{R_\mathrm{c}}\right)\right) \tag{2}$$

with θ the peeling angle, s_0 the abscissa for the clamping condition and R_c the radius of curvature of the backing of the tape. Moreover the radius of curvature is directly linked to the geometry of the backing of the tape and its Young's modulus E_back:

$$R_\mathrm{c} = \sqrt{\frac{E_\mathrm{back}be^3}{12F(1-\cos\theta)}} \tag{3}$$

with $b = 19\,\mathrm{mm}$ the width of the tape and $e = 38\,\mathrm{\mu m}$ the thickness of the backing of the tape.

In Fig. S2, the extracted radius of curvature R_c is represented as a function of the applied load $F(1-\cos\theta)$ for different humidities. The radius of curvature R_c follows the equation (3), scaling as the inverse of the square root of the applied load.

The Young's modulus E_back of the backing of the tape for different humidities can be extracted as shown in Fig.S 3. The Young's modulus is almost independent of the relative humidity: we find $\langle E_\mathrm{back}\rangle = 1.44 \pm 0.26\,\mathrm{GPa}$, in good agreement with values from the literature [2, 3]. We conclude that the impact of the relative humidity on the peeling velocity is due to change in the adhesive and not in the properties of the backing of the tape.
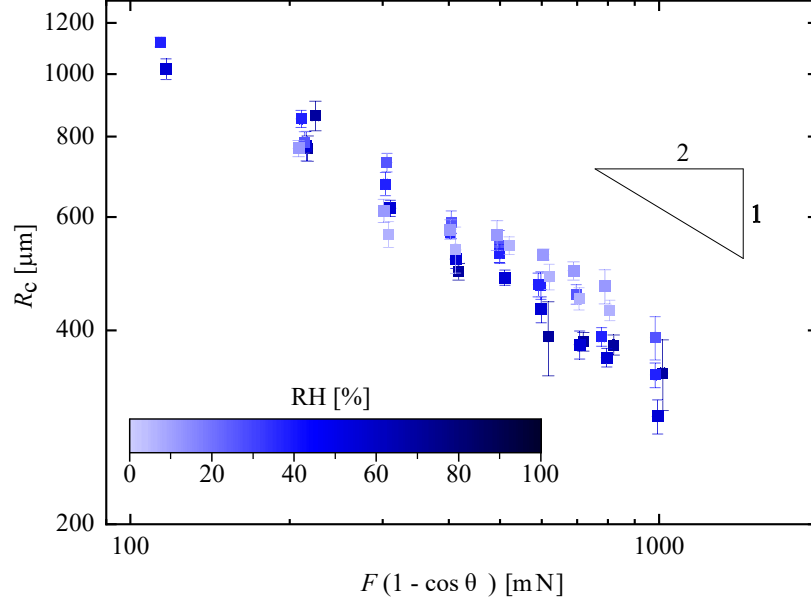
FIG. S2. Radius of curvature R_c of the backing of the PSA as a function of the applied force $F(1 - \cos\theta)$. The color scale indicates the different relative humidity RH.
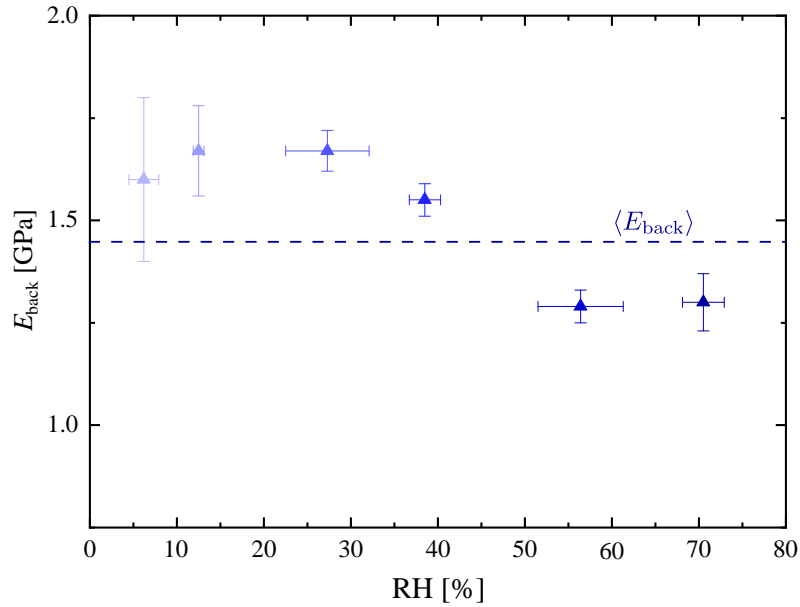

FIG. S3. Young's modulus E_{back} of the backing of the PSA as a function of the relative humidity RH. The dotted line represents the mean value $\langle E_{back} \rangle = 1.44\,\text{GPa}$.

II.   PEELING EXPERIMENTS AT DIFFERENT RELATIVE HUMIDITIES

For the sake of clarity, only part of the peeling data are presented in Fig. 2(a). In Fig. S4, we present all the data used to construct the peeling master curve presented in Fig. 2(b).
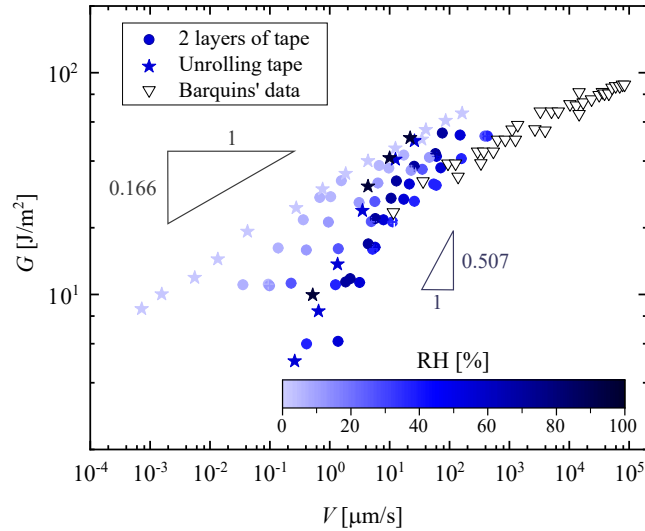

FIG. S4. Strain energy release rate G as a function of the peeling velocity V of the adhesive for the unrolling tape and the two layers of the adhesive. The color map indicates the different relative humidity RH. We also plot Barquins' data [4] for the subcritical crack growth mode.

The peeling master curve (Fig. 2(b)) is obtained by tuning the rescaling factor $a_{\mathrm{RH}}(\mathrm{RH})$. In Fig. S5, a_{RH} is shown to decrease with RH.
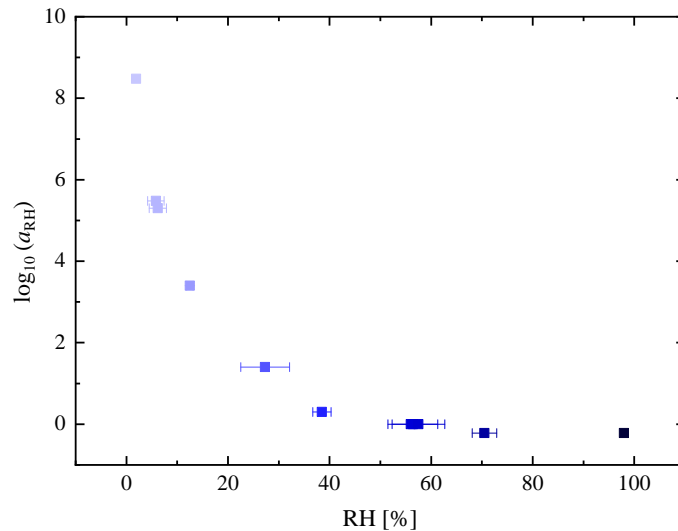

FIG. S5. Rescaling factor a_{RH} that allows for the collapse of the data, i.e. to construct the master curve in Fig. 2(b) as a function of the relative humidity RH.

III.   ABSORPTION OF WATER BY THE ADHESIVE LAYER

In order to connect the RH to the adhesion characteristics of the Scotch tape material, we measure the amount of water absorbed by the hygroscopic adhesive as a function of RH by using a simple gravimetric test. Samples of tape of one meter long are dried in a sealed box under a nitrogen flow at ambient temperature for several days. The dried samples are then exposed to different relative humidity for typically 2 days, to ensure the saturation of absorption of water. The water content for each relative humidity is deduced by weighing the samples (Mettler Toledo MS205DU, accuracy 0.01 mg). The percentage of water content, W_c, is determined by $W_c = \frac{M_f - M_0}{M_0} \times 100$, where M_f and M_0 are the weights of wet and dried specimens, respectively.
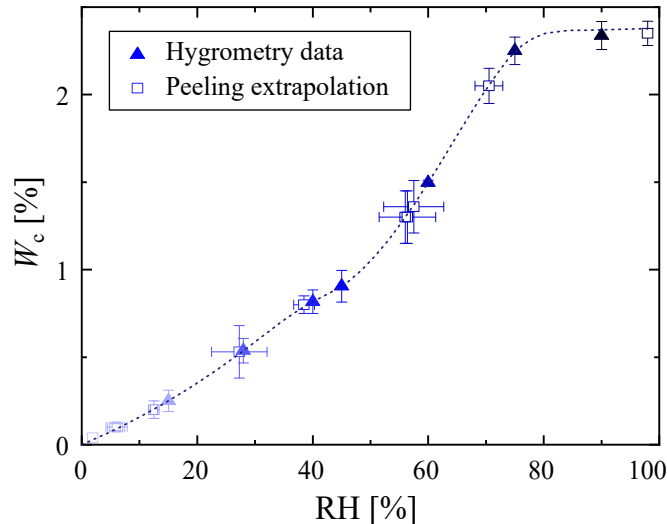

FIG. S6. Water content in the adhesive W_c measured by gravimetric test (triangle) as a function of the relative humidity RH. The dotted line is a spline interpolation used to extrapolate the water content corresponding to the peeling experiments (square).

In Fig. S6, the water uptake is shown to increase non-linearly with the relative humidity. At high humidity, W_c reaches more than 2.35%. We used a spline interpolation (dashed line) on the hygrometry data to extrapolate the water content corresponding to the peeling experiments (square symbols).

IV. IR SPECTROPHOTOMETRY

IV.1. Comparison between tapes 3M 810 and 600

A Bruker Vertex 70 FTIR spectrometer (Bruker, Billerica, MA) is used to measure the 1D-IR (FTIR). The absorption spectra were recorded at a wavenumber resolution of $2\,\mathrm{cm}^{-1}$. We averaged 32 scans for every spectrum. We compare three samples: the tape 3M 810 at ambient RH (RH$\sim$ 50%), the same tape dried for 5h under a nitrogen flow (RH$<$ 1%) and the tape 3M 600 at ambient RH, used by Barquins *et al.* [4]. Fig. S7(a) compares the spectra of the three samples.
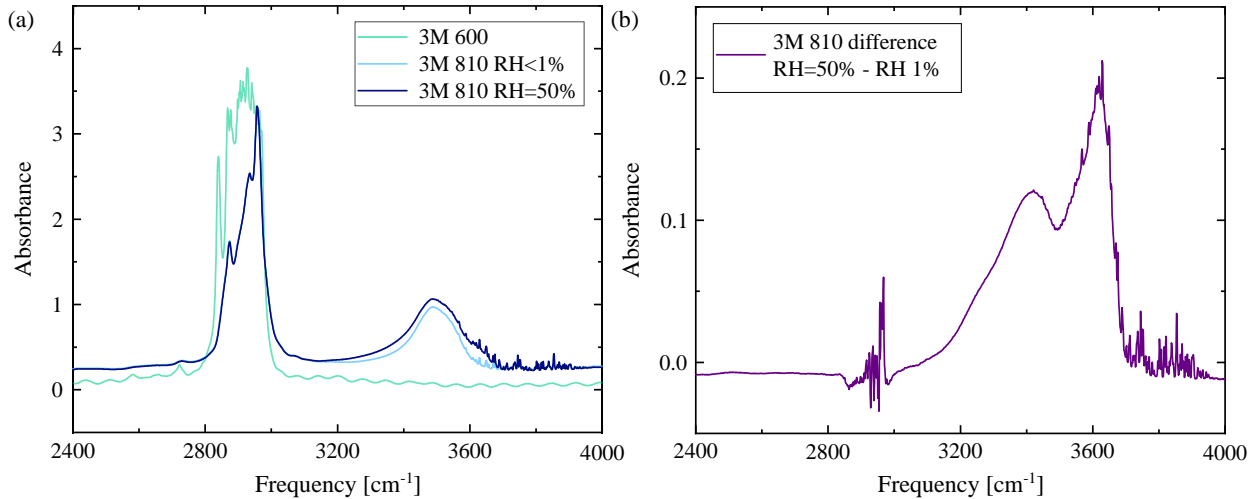

FIG. S7. (a) IR-spectra of the tape 3M 810 at ambient RH (RH$\sim$ 50%) and dried (RH$<$ 1%) and the tape 3M 600 at ambient RH. (b) Difference of the IR-spectra for the wet and dried tape 3M 810.

Scotch tape 3M 810 presents a broad peak around $3400\,\mathrm{cm}^{-1}$ due to OH stretching for both the dried and the ambient RH samples. We still observe the OH peak after 5h of drying, indicating this remaining peak must be due to OH side groups in the tape. Fig. S.7(b) presents the difference spectrum between the ambient RH and the dried samples: the double OH-peak agrees with the spectrum of H_2O in organic environment [5]. This clearly indicates the presence of water in the adhesive at ambient RH and confirms that the mass uptake we measured by gravimetric test is indeed water uptake.

The IR-spectrum of Scotch tape 3M 600 reveals the different chemistry of this tape compared to 3M 810 as there is no peak around $3400\,\mathrm{cm}^{-1}$, indicating the complete absence of water and OH side groups. This explains why Barquins *et al.* did not report any effect of the humidity on the peeling of this tape.

IV.2. Drying of the tape 3M 810

On top of the mechanical changes in the tape, water may alter the interactions between the polymer chains in the adhesive [6]. In order to investigate this effect, we dried the tape 3M 810 in the spectrometer, taking IR spectra each 2 min as described above.
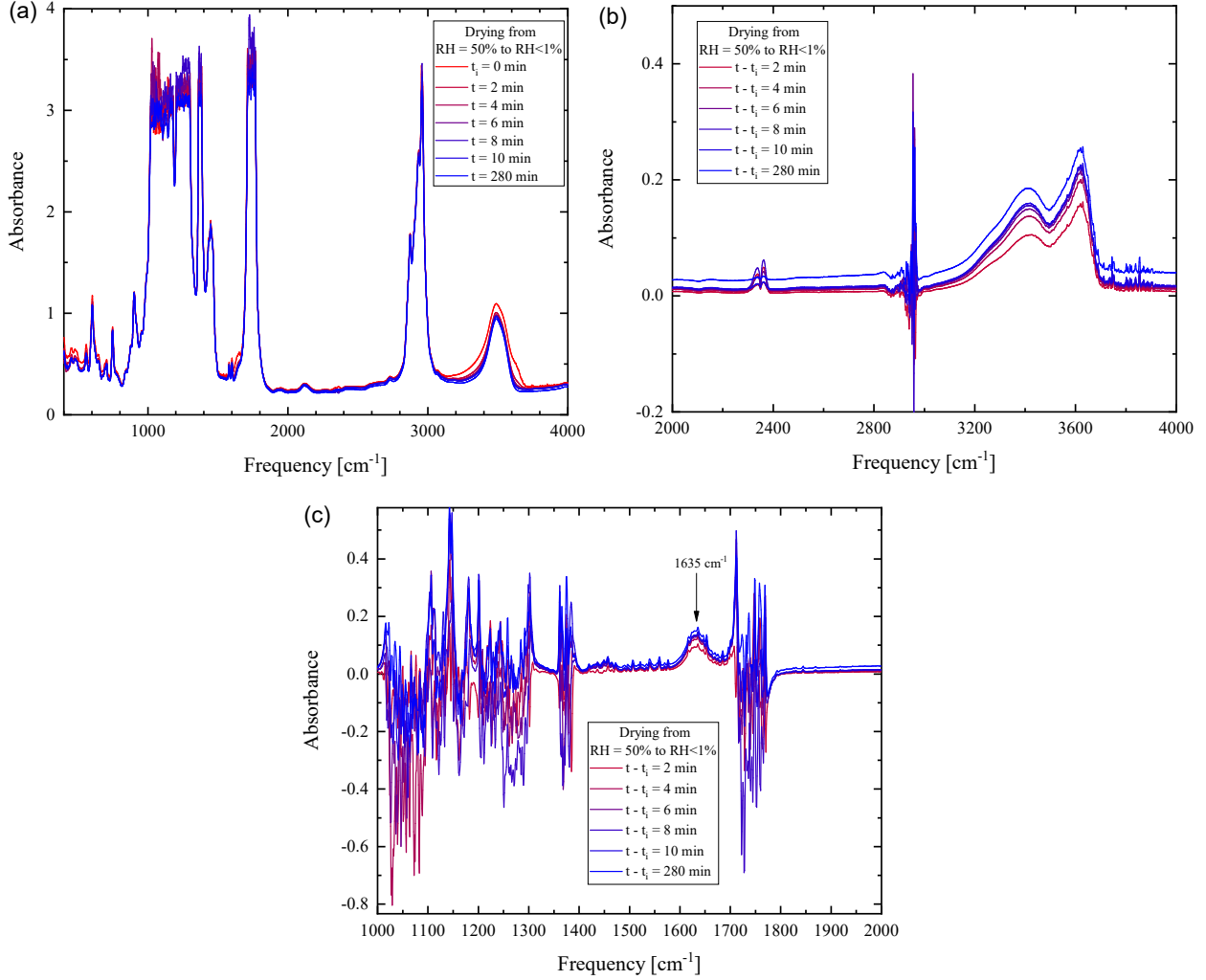

FIG. S8. (a) IR-spectra of the tape 3M 810 at ambient RH (RH$\sim$ 50%, $t_i = 0$ min) and drying down to RH$< 1\%$ at $t = 240$ min. (b) and (c) Difference of the IR-spectra for the wet and dried tape 3M 810 at different drying time.

As shown in Fig. S8(a), the IR-spectra of the drying tape differ systematically with the drying time for two specific peaks, respectively around $3400\,\mathrm{cm}^{-1}$ (see Fig. S8(b)) and $1635\,\mathrm{cm}^{-1}$ (see Fig. S8(c)). The peak at $3400\,\mathrm{cm}^{-1}$ has been described above as the one of H_2O in organic environment [5]. The peak around $1635\,\mathrm{cm}^{-1}$ is due to H_2O scissors bending vibration of water [7]. As these changes in the IR-spectra are both due to water, the IR spectra indicates that other secondary interactions in the polymer chains are negligible.

V. CALCULATION OF THE VELOCITY OF PEELING FROM RELATIVE HUMIDITY MEASUREMENTS

Based on the time-humidity superposition principle and the peeling master curve, it is possible to calculate the evolution of the velocity of peeling $V(t)$ of the tape in time knowing the evolution of the relative humidity. Here we detail how we proceeded to calculate $V(t)$ in Fig. 1(b) (red line) based on the measurements of $\mathrm{RH}(t)$.

The peeling master curve presented in Fig. 2(b) is fitted around the range of the data for the peeling experiment over a month: $b_{\mathrm{RH}}G_{1\,\mathrm{month}} \in [10^0 - 10^6]\,\mathrm{J/m^2}$. This part of the data can be fitted as double power law:

$$b_{\mathrm{RH}}G = \begin{cases} \beta(a_{\mathrm{RH}}V)^{\alpha_1}, & \text{if } \mathrm{RH} \geq \mathrm{RH}_{\mathrm{cut}} \\ \beta(a_{\mathrm{RH}}V)^{\alpha_2}(b_{\mathrm{RH}}(\mathrm{RH}_{\mathrm{cut}})G/\beta)^{\frac{\alpha_1-\alpha_2}{\alpha_1}}, & \text{otherwise} \end{cases}$$

Figure S9 presents the best double power law fit (red line), with $\mathrm{RH}_{\mathrm{cut}} = 25.3\%$, $\alpha_1 = 0.60 \pm 0.23$, $\alpha_2 = 0.216 \pm 0.005$ and $\beta = 9.73 \pm 3.43\,10^{-6\alpha_1}\,\mathrm{J}^{\alpha_1}\mathrm{s}^{\alpha_1}/\mathrm{m}^{\alpha_1}$.
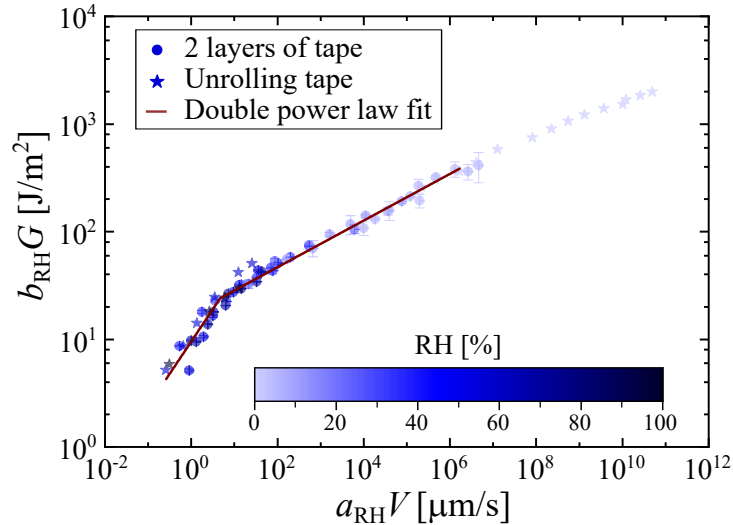

FIG. S9. Double power law fit of the peeling master curve with $\mathrm{RH}_{\mathrm{ref}} = 56.7\%$. The rescaled strain energy release rate $b_{\mathrm{RH}} \cdot G$ (with $b_{\mathrm{RH}} = \mathrm{RH}_{\mathrm{ref}}/\mathrm{RH}$) is plotted against the rescaled peeling velocity $a_{\mathrm{RH}} \cdot V$. The red line is the best double power law fit.

For the experiment over a month, b_{RH} is measured, the strain energy release rate is considered constant $G \sim 10.8\,\mathrm{J/m^2}$. To calculate $V(t)$ with the fit of the peeling master curve presented above, we need to extrapolate the rescaling factor a_{RH} from the measurements of RH. In Fig. S10(a), the same spline interpolation (dashed line) on the hygrometry data (blue symbols) as in Fig. S6 is used to extrapolate the water content $W_{\mathrm{c}}(t)$ corresponding to the peeling experiments over a month (square symbols).

These extrapolated values of water content $W_{\mathrm{c}}(t)$ are then used to calculated with the time-humidity superposition principle (Eq. (1)) the rescaling factor $a_{\mathrm{RH}}(t)$ for the peeling experiment over a month (see Fig. S10(b)).
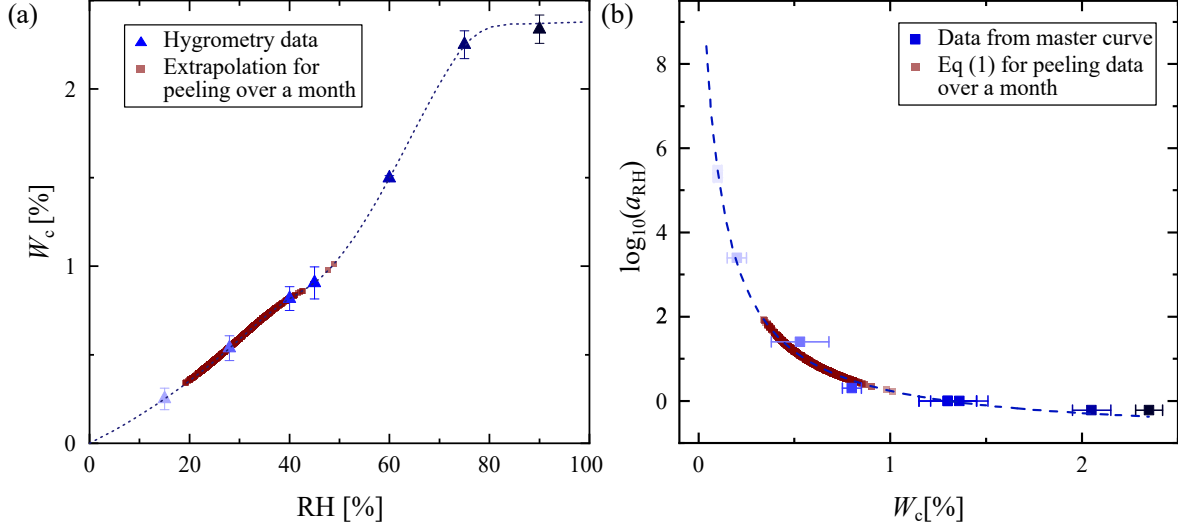
FIG. S10. (a) Extrapolation of the water uptake for the peeling experiment over a month (red) based on the hygroscopic data (blue) with the relative humidity data from Fig. 1(b). (b) Calculation of the rescaling factor a_{RH} for the peeling experiment over a month (red) with the equation (1). Blue points are the data from the peeling experiments with different forces, presented in Fig. 2(c).

Last, with the fit of the peeling master curve and the time-humitidy superposition principle, the velocity of peeling $V(t)$ over a month can be calculated, as presented in Fig. 1(b) (red) and shown again in Fig. S11 for sake of clarity. Calculated values are in good agreement with the experiment data, revealing the accuracy of the peeling master curve.
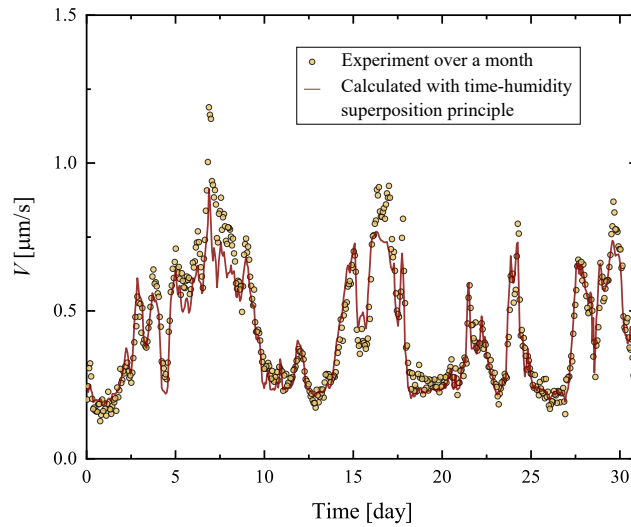

FIG. S11. Unrolling of a suspended roll of tape over a period of one month. Velocity of peeling V of the roll of tape as a function of time. The red line is the velocity of peeling calculated for the time-humidity superposition principle.

9

VI. STRETCHING OF FIBRILS

As shown in Fig. S1(a), complex fibrils also form around the debonding region in our peeling experiments. The maximum fibril stretch ϵ_f is defined as $\ln(a_f/e)$, with a_f the maximal fibril length at debonding and $e = 28\,\mu m$ the thickness of the adhesive. Fig.S12 shows the maximum fibril stretch ϵ_f at debonding as a function of the peeling velocity V for two different relative humidities. Within the limitations of our setup, the stretching of the fibrils seems to be independent of the peeling velocity V and the relative humidity.
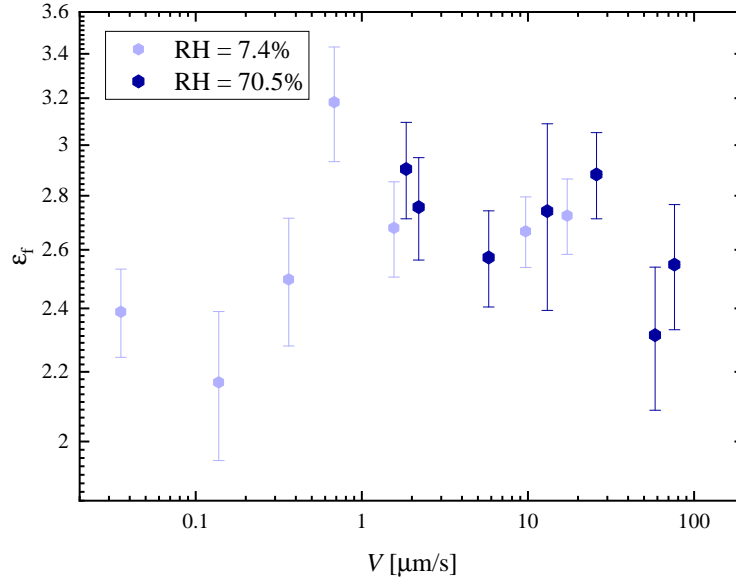

FIG. S12. Maximum fibril stretch ϵ_f at debonding as a function of the peeling velocity V for two different relative humidities

Chopin *et al.* [8, 9] recently showed that the adherence curve $G(V)$ presents two contributions: a rate-dependent linear viscoelastic factor and a nonlinear factor linked to the fibril stretching. They showed that a polymer for which the stretching of the fibrils is rate independent, the adherence curve is mainly due to linear viscoelastic rheology. As the tape we studied also presents a rate independent stretching of the fibrils, the linear viscoelasticity dominates in the adherence curve. Thus, the 'time-humidity' superposition principle is applicable to rationalize the peeling experiments. Note that the same rate independence of the stretching of fibrils have been reported for the Scotch tape 600 by Villey [10], allowing us to compare the peeling mechanism of the tape 810 to this one.

[1] A. E. H. Love, *A Treatise on the Mathematical Theory of Elasticity* (Cambridge University Press, 1944).

[2] A. Molinari and G. Ravichandran, The Journal of Adhesion **84**, 961 (2008).

[3] C. Kovalchick, *Mechanics of Peeling: Cohesive Zone Law and Stability*, phd, California Institute of Technology (2011).

[4] M. Barquins and M. Ciccotti, International Journal of Adhesion and Adhesives **17**, 65 (1997).

[5] V. V. Troshin, L. A. Sheludyakova, and I. V. Mironov, Journal of Analytical Chemistry **63**, 544 (2008).

[6] J. E. Huacuja-Sánchez, K. Müller, and W. Possart, International Journal of Adhesion and Adhesives **66**, 167 (2016).

[7] A. Célino, O. Gonçalves, F. Jacquemin, and S. Fréour, Carbohydrate Polymers **101**, 163 (2014).

[8] J. Chopin, R. Villey, D. Yarusso, E. Barthel, C. Creton, and M. Ciccotti, Macromolecules **51**, 8605 (2018).

[9] R. Villey, C. Creton, P.-P. Cortet, M.-J. Dalbe, T. Jet, B. Saintyves, S. Santucci, L. Vanel, D. J. Yarusso, and M. Ciccotti, Soft Matter **11**, 3480 (2015).

[10] R. Villey, P.-P. Cortet, C. Creton, and M. Ciccotti, International Journal of Fracture **204**, 175 (2017).